Biointerphases
A Journal of Biomaterials and Biological Interfaces

ARTICLE

avs.scitation.org/journal/bip

Evaluation of surface layer stability of surface-modified polyester biomaterials

Cite as: Biointerphases 15, 061010 (2020); doi: 10.1116/6.0000687
Submitted: 1 October 2020 · Accepted: 5 November 2020 ·
Published Online: 4 December 2020

Hamish Poli,[1] Alexandra L. Mutch,[1] Anitha A,[1] Saso Ivanovski,[2] Cedryck Vaquette,[2] David G. Castner,[3] María Natividad Gómez-Cerezo,[2,a)] and Lisbeth Grøndahl[1,4,b)]

AFFILIATIONS

[1]School of Chemistry and Molecular Biosciences, The University of Queensland, St Lucia 4072, Australia
[2]School of Dentistry, The University of Queensland, Herston 4006, Australia
[3]Department of Bioengineering and Department of Chemical Engineering, National ESCA and Surface Analysis Center for Biomedical Problems, University of Washington, Seattle, Washington 98195
[4]The Australian Institute for Bioengineering and Nanotechnology, The University of Queensland, St Lucia 4072, Australia

Note: This paper is part of the Biointerphases Special Topic Collection on Biointerface Science in Australia 2020 - An issue in celebration of Hans Griesser's career.

[a)]**Electronic mail:** m.gomezcerezo@uq.edu.au
[b)]**Electronic mail:** l.grondahl@uq.edu.au

ABSTRACT

Surface modification of biomaterials is a strategy used to improve cellular and *in vivo* outcomes. However, most studies do not evaluate the lifetime of the introduced surface layer, which is an important aspect affecting how a biomaterial will interact with a cellular environment both in the short and in the long term. This study evaluated the surface layer stability *in vitro* in buffer solution of materials produced from poly(lactic-co-glycolic acid) (50:50) and polycaprolactone modified by hydrolysis and/or grafting of hydrophilic polymers using grafting from approaches. The data presented in this study highlight the shortcomings of using model substrates (e.g., spun-coated films) rather than disks, particles, and scaffolds. It also illustrates how similar surface modification strategies in some cases result in very different lifetimes of the surface layer, thus emphasizing the need for these studies as analogies cannot always be drawn.

I. INTRODUCTION

The applications of polyester-based materials in biomedicine as nanoparticles, films, and scaffolds have been widely explored in past decades due to the biodegradability of these materials.[1–5] However, their high hydrophobicity limits their applications in biomedicine as it affects the protein adhesion and therefore the immune response and cell behavior to those polymers *in vivo*. For this reason, the modification of the surface by different strategies such as hydrolysis, plasma treatment, and photo or gamma irradiation-induced grafting has been widely studied.[6–8] Various studies have evaluated changes to surface properties,[6,8] changes to bulk properties including bulk degradation and mechanical properties,[9] *in vitro* cell attachment,[10–12] and *in vivo* response and degradation.[13] However, one aspect that to a large extent is overlooked is that the introduced surface layer may have a very different lifetime to that of the bulk polymer, and only a few studies have reported this.[14–16] Thus, most previous studies have not explored the behavior of the surface itself during degradation, cell growth, or *in vivo*.

There are two potential scenarios that can be envisaged when there is a mismatch between surface and bulk degradation.[14] In the first scenario, an essentially nondegradable surface layer is introduced on a degradable biomaterial. As the biomaterial degrades, the surface layer is left behind. One example of how such a situation could arise is if a crosslinked plasma polymer film with high stability[17,18] is deposited on a biodegradable polyester biomaterial. In the second scenario, a surface layer is introduced that degrades much more rapidly than the bulk material. This scenario potentially introduces a number of unwanted issues. First, a very unstable surface layer will potentially affect measurements of the water contact angle, for example, due to oligomers from the surface layer

dissolving into the droplet during contact angle measurements, as has been previously highlighted for oxygen plasma-treated substrates where insufficient washing prior to contact angle measurements led to erroneous results.[19] Second, during cell culture and *in vivo* experiments, a large proportion of the surface layer may be displaced before a cellular and tissue response ensues.

There is thus a need to address this knowledge gap in evaluating the longevity of surface layers, in general, and specifically for surface-modified polyester biomaterials. The key to such evaluation is in-depth surface characterization, which includes the evaluation of changes in chemical composition, changes in wettability, and changes in surface roughness.[20,21] A number of studies have evaluated changes to surface properties during degradation.[22–24] However, only a few have evaluated the stability of introduced surface layers. One such previous study evaluated the effect of aminolysis of polycaprolactone (PCL) using x-ray photoelectron spectroscopy (XPS) and found an 80% reduction in surface amine groups after immersion in aqueous buffer at 37 °C for 3 days.[15] It must be appreciated that the nature of the substrate plays an essential role in terms of suitable surface characterization methods.[25] For example, the study of complex structures such as scaffolds affords additional challenges and limits the choice of suitable characterization techniques.

In the current study, the surface layer stability of a series of polyester-based substrates produced from either PCL or poly (lactic-co-glycolic acid) (PLGA) was evaluated *in vitro* in buffer solution. These included spun-coated and melt-pressed disks, particles, and melt-electrowritten scaffolds. The surface modification techniques evaluated were hydrolysis, grafting of an amino acid, and graft copolymerization which all introduced functional groups onto the surface of the materials. Evaluation of the surface layer stability was done using a range of surface analysis techniques, for example, XPS, atomic force microscopy (AFM), and water contact angle measurements, as well as techniques specific to certain substrates, for example, dynamic light scattering (DLS) and scanning electron microscopy (SEM). The combined data have allowed a thorough evaluation of certain systems and the identification of limitations for other systems. The data and conclusions presented here will help guide future studies on the surface layer stability of surface-modified polyester-based materials.

II. MATERIALS AND METHODS

A. Materials

Medical grade polycaprolactone (PCL) (Purasorb® PC 12, viscosity midpoint 1.2 dl g^{-1}, M_w = 120 kg mol^{-1}) was purchased from Corbion. Poly(lactic-co-glycolic acid) (PLGA, Resomer® RG 502H, acid terminated, L:G = 50:50; Mw = 7–17 kg mol^{-1}), 2-aminoethyl methacrylate hydrochloride (AEMA, 90%, stabilized with 500 ppm phenothiazine) and 3-sulfopropyl acrylate sodium salt (SPA) were purchased from Sigma Aldrich. Silicon wafers (10 × 10 × 1 mm, orientation ⟨100⟩, P-type doped, 1 ∼ 50 Ω cm) were supplied by the Australian National Fabrication Facility, Queensland, and New South Wales Nodes. Phosphate-buffered saline (PBS) tablets were purchased from Invitrogen. Ammonium iron(II) sulfate hexahydrate (Mohr's salt) (99%), Nα-(*tert*-butoxycarbonyl)-L-lysine [L-lysine(Boc)] (99%), trimethylchlorosilane (TMCS) (≥98%), N-hydroxysuccinimide (NHS) (98%), N-(3-dimethylaminopropyl)-N′-ethylcarbodiimide hydrochloride (EDC) (98%), and anisole (anhydrous, 99.7%) were purchased from Sigma Aldrich. n-hexane and dichloromethane (DCM) were purchased from Merck. Ammonia solution (28%) and hydrogen peroxide (30%) were purchased from Chem-Supply. Pentafluorophenol (PFP) was purchased from FluoroChem. Ultrapure (UP) water was obtained through a VWR International PureLab Flex ELGA purification system (18.2 MΩ).

B. Substrate preparation

Particles were prepared from a 20 mg ml^{-1} PLGA solution (0.5 ml) in DCM that was added dropwise to a 20 mg ml^{-1} PVA in UP water solution (2 ml) while stirring. The emulsion was sonicated on ice with a Branson Digital Probe Sonifier 450 for 90 s at 10% amplitude, diluted to 50 ml of UP water, and stirred for 3 h to evaporate DCM. The solution was divided into 8 ml aliquots which were centrifuged at a relative centrifugal force of 76 500×g for 1 h.

Silicon wafers were cleaned with a piranha solution containing UP water, hydrogen peroxide (30%), and ammonia (28%) in a 5:1:1 volume ratio. *Caution! Piranha solution reacts violently with organic materials and must be handled with care*. Each silicon wafer was placed into a Pyrex test tube containing 2.8 ml of the piranha solution and test tubes were immersed in water at 80 °C for 20 min. The wafers were then removed from the solutions and rinsed three times each in UP water (approximately 20 ml) before being dried under a stream of N_2. Immediately after piranha treatment, each wafer was silanized using a solution of TMCS in hexane (5% v/v). Each wafer was placed into a Pyrex test tube containing 2 ml of TMCS solution and left at room temperature for 10 min. The wafers were then rinsed three times each in hexane (approximately 20 ml) before being dried under a stream of N_2.

Spin-coated polymer films were prepared by covering silanized wafers with a 2% (w/v) anisole solution of polymer (PCL or PLGA). For PLGA samples, the solution was filtered through a PTFE syringe filter (0.45 μm) onto the Si wafers. For PCL samples, the solution was left on the wafer for 2 min before spinning. Spin coating was carried out using a CHEMAT Technologies KW-4A spin coater. PLGA samples were obtained by spinning for 6 s at 250 rpm followed by 40 s at 1000 rpm, yielding $PLGA_f$. PCL samples were obtained by spinning for 3 s at 300 rpm followed by 20 s at 1000 rpm, yielding PCL_f.

Melt-pressed PCL disks were prepared by placing PCL pellets (4–6 g) on top of a sheet of borosilicate glass (100 × 100 × 3 mm^3) on a hotplate. The pellets were placed as close together as possible and the hotplate was set to 150 °C. The pellets were left to melt for 15 min before the glass and sample were removed from the hotplate to cool to room temperature. The glass and sample were then placed back on the hotplate and a second borosilicate glass sheet was placed on top of the sample to flatten it. The hotplate was again set to 150 °C to remelt the sample. After 5 min, a 1.2 kg weight was placed on top of the glass sheet to compress the sample, which was heated for a further 10 min with the weight on top. The sample was then removed from the hotplate and left between the glass sheets overnight to cool. The PCL disks were approximately 1.5–2.0 mm thick and cut into approximately 8 × 8 mm^2 squares, washed in water overnight before being dried by a stream of N_2, and stored in a desiccator, obtaining PCL_d samples.

PCL melt-electrowritten scaffolds were fabricated via a direct writing approach,[26] whereby a programmable x-y stage is used to collect the fibers. Briefly, PCL pellets were placed into a 2 ml syringe and heated at 80 °C in an oven to melt the polymer. The polymer was printed through a blunt 21 G needle, at a pressure of 160 mPa, a voltage of 8 kV, and a spinneret collector distance of 8 mm. The temperatures of heater #1 (placed near the syringe) and heater #2 (placed near the needle) were set to 75 and 85 °C, respectively. The translational speed of the collector was 850 mm min^{-1}, obtaining straight fibers. A square wave pattern was utilized to manufacture scaffolds printing alternating layers oriented at 0–90° with a 500 μm fiber interdistance. The scaffold (0.5 mm thickness) was sectioned into 5 mm, using a biopsy punch, obtaining the substrates as PCL_s.

C. Surface modification

Hydrolyzed samples were prepared by alkaline hydrolysis. The PCL_s samples were immersed in 3 M NaOH for 90 min at 37 °C under constant stirring at 100 rpm. The scaffolds were thereafter rinsed several times in distilled water to remove any excess of NaOH, yielding h-PCL_s. The $PLGA_f$ samples were submerged in 5 ml of 2.5 mM NaOH for 3 h under mild shaking after which they were removed, washed in UP water (×3), and dried under a stream of N_2, yielding h-$PLGA_f$. Hydrolysis of the $PLGA_p$ was done by resuspending the particle pellet in 10 ml of 2.5 mM NaOH and stirring for 3 h and centrifuged as described above to form h-$PLGA_p$.

Graft copolymerization of the monomers AEMA and SPA was achieved by placing each substrate (PCL_f or PCL_d) into a separate test tube containing 2 ml of the monomer solution (20% w/v) in UP water. Samples grafted with SPA also had Mohr's salt 1% (w/v) added to minimize homopolymer formation. The test tubes were sealed with SubaSeal stoppers and left overnight for solvent uptake into the substrates. Before irradiation, the tubes were flushed with N_2 gas for 10 min (approximately 4 ml min^{-1}) to remove dissolved oxygen. The test tubes were then irradiated with a ^{60}Co gamma radiation source (Nordion GammaCell 220) at 420–433 Gy h^{-1} to a total dose of 2 kGy. After irradiation, the grafted PCL samples were washed in UP water (100 ml) for 1 min with stirring, followed by washing in 20 ml of UP water for 1 h twice, and then finally overnight in a further 20 ml of UP water. The grafted PCL samples were then dried by a stream of N_2 and stored in a desiccator. This process yielded the following samples a-PCL_f or a-PCL_d when grafted with AEMA and s-PCL_f or s-PCL_d when grafted with SPA.

Hydrolyzed PCL_s samples were rinsed twice with UP water (20 ml) for 5 min before they were suspended in 1.0 ml of aqueous solution containing EDC:NHS:L-lysine(Boc) 2:1:1 molar ratio in water (39, 12, and 11.8 mg, respectively). The suspension was stirred for 6 h at room temperature. The resulting samples were rinsed twice with UP water and dried under vacuum, yielding L-PCL_s.

D. Stability evaluation

Phosphate-buffered saline (PBS, 10 mM phosphate, 150 mM sodium chloride, *p*H 7.5) was used for stability evaluation. Each solid sample was immersed in 10 ml of PBS solution and placed in a shaking water bath at 37 °C for varying time points up to 21 days. The *p*H of the solution was found not to change over the course of this study. The samples were then washed with UP water until the washed solution no longer produced a precipitate upon the addition of $AgNO_3$ (0.1 M). The samples were then dried under a stream of N_2 before being stored in a desiccator for at least two days. The stability of $PLGA_p$ and h-$PLGA_p$ was assessed by resuspending the pellets in PBS. Some select samples were also evaluated in UP water in a similar manner to that described for PBS. The PCL_f was observed in some cases to delaminate from the silicon wafer after 10+ days in PBS, with some samples being completely delaminated after immersion. Samples with no film remaining on them were not analyzed by contact angel (CA) or XPS. All samples were run in duplicate.

E. Characterization

Ellipsometry was used to analyze the thickness of $PLGA_f$. A J.A. Woollam M-2000 Ellipsometer (automated angle, horizontal) operating with variable angle spectroscopic ellipsometry (VASE) was used to measure Ψ and Δ at 60°, 65°, 70°, and 75°. Model parameters were automatically fitted using a Cauchy model of PLGA (A = 1.49) on a silicon substrate. Thin film thickness was measured at five spatial locations on the 2D surface. Duplicate samples were measured. Films for which the mean squared error value was greater than 10 were not included.

CA measurements were performed by using a DataPhysics Instruments OCA 14EC/B Contact Angle Measurement Instrument. All samples were washed thoroughly prior to the CA measurements. For each measurement, 5 μl of UP water was dispensed onto the surface and the contact angles were calculated by an ellipse fitting method using the DataPhysics SCA202 software. Each sample was analyzed by depositing four drops at different locations and each sample was evaluated in duplicate, resulting in 16 CA measurements, unless otherwise stated.

X-ray photoelectron spectrometry (XPS) was used to evaluate the surface composition, using a Kratos Axis ULTRA x-ray photoelectron spectrometer incorporating a 165 mm hemispherical electron energy analyzer. The incident radiation was monochromatic Al Kα X-rays (1,486.6 eV) at 150 W (15 kV, 10 mA). Survey (wide) scans were taken at an analyzer pass energy of 160 eV and multiplex (narrow) high resolution scans at 20 eV. Survey scans were carried out over a 1200–0 eV binding energy range with 1.0 eV steps and a dwell time of 100 ms. Narrow high-resolution scans were run with 0.05 eV steps and a 250 ms dwell time. The base pressure in the analysis chamber was 10^{-9} Torr and during the sample analysis it was 10^{-8} Torr. Atomic concentrations were calculated using the CasaXPS version 2.3.14 software and a Shirley baseline with Kratos library Relative Sensitivity Factors. The samples were run in duplicate and one spot on each sample was analyzed. Peak fitting of the high-resolution data was also carried out using the CasaXPS software. All high-resolution scans were charge-corrected to the C*–C peak at 285.0 eV. Some samples were treated with a PFP probe to quantify the amount of carboxyl groups present on the surface.[9] For this, a 3:1 solution containing EDC (135 mg, 704 μmol) and PFP (43.3 mg, 235 μmol) was prepared in UP water. From this solution, each sample was submerged in a 5 ml aliquot with continuous shaking (1 h, 1–4 °C) and then at room temperature for 3 h. The samples were then washed in UP water (×3) and dried under a stream of N_2. Piranha and TMCS

treated silicon wafers which were subsequently treated with PFP served as control samples. The theoretical Si/C ratio of 1.9 for the silanized silicon wafers represents the expected outcome after the polymer has been eroded from surface, and therefore, any sample that displayed Si/C ratios of or above this theoretical value was not included for analysis and discussion.

Atomic force microscopy (AFM) was used to evaluate the surface roughness at ambient conditions with an Asylum Research Cypher S Microscope in AC mode (controlled with AR 16.10 software). Commercially available silicon cantilevers (TipsNano) with a typical resonance frequency of 235 kHz/140 kHz and a typical force constant of 12 N m^{-1}/3.5 N m^{-1} were used. The set point and drive amplitude were optimized to reduce tip–sample interactions. Images were captured in a 400 or 25 μm^2 area with 512 trace lines and at a scan rate of 1–1.6 Hz. Surface height profiles were drawn diagonally across the images and the median plane was normalized to 0 nm. The average roughness (R_a) was calculated as the average height deviation from the mean plane over a 16 μm^2 area unless otherwise stated.

Dynamic light scattering (DLS) measurements were performed on a Malvern ZetaSizer Nano ZS 3600 at 25 °C in water or PBS ($\eta = 0.8872$ cP, n(or RI) = 1.33). The refractive index of PLGA was 1.49 across all samples. The angle of detection was set to 173° in backscatter. Each sample was measured in triplicate.

Scanning electron microscopy (SEM) imaging was carried out using a JSM F-7001 microscope (JEOL Ltd., Tokyo, Japan). The samples were mounted onto SEM stubs and carbon-coated in a vacuum using a sputter coater (Quorum Q150 T carbon coater, Quorum Technologies Inc.).

F. Statistical analysis

Statistical analysis was completed using GrahpPad Prism 8.2.1. For measurements where three or more data were obtained this was done using Ordinary two-way ANOVA. For comparing the same type of sample immersed at different time points: Tukey's multiple comparisons test, with individual variances was computed for each comparison. For comparing different types of samples at the same immersion time: Sidak's multiple comparisons test, with individual variances was computed for each comparison. Samples are considered significantly different when $p < 0.05$. XPS data including atomic ratios are considered significantly different between the samples when the difference is greater than 10%.

III. RESULTS AND DISCUSSION

A. Surface modification

Two different polyesters were chosen for this study: PLGA (50:50) and PCL. They differ with regard to crystallinity, hydrophobicity, and degradation rate and mechanism. Specifically, PLGA is an amorphous[27,28] random copolymer with a T_g of 46 °C[29] that undergoes bulk degradation.[23] PCL is a highly crystalline polymer (a crystallinity of 50%–72%) with a T_g of −60 °C.[22] It is hydrophobic with reported contact angles ranging from 75° to 91°,[9,30] and the water uptake is negligible at neutral *p*H.[1,9]

From each polyester different substrates were prepared, specifically particles, spun-coated films, melt-pressed disks, and melt-electrowriting scaffolds as outlined in Table I. The spun-coated films represent a model system for which extensive characterization can be done including contact angle measurements, ellipsometry, and AFM. Scaffolds used in tissue engineering can be prepared using solvent-based processes (e.g., electrospinning) or melt-based processes (e.g., 3D printing and melt-electrowriting). As such, the melt-pressed disks are included to evaluate any difference in surface modification and/or degradation between solvent- and melt-based materials. The melt-electrowritten scaffolds are an example of a final complex structure. Thus, while some of the selected substrates are model substrates, others have potential applications in biomedicine including drug delivery using particles and tissue engineering using scaffolds. Drug delivery systems based on the particles of PLGA and other systems in the size range of 50–200 nm are preferred for nanomedicine applications including cancer treatment.[31] As such, improved circulation half-life is required for these types of systems to be effective,[5] and therefore, the present study evaluated this for 3 weeks. Furthermore, melt-electrowriting scaffolds display an interconnected pore structure with controlled porosity, pore morphology, and pore size, allowing optimization of cell infiltration and subsequent vascularization and angiogenesis, making this type of scaffold very suitable for the regeneration of soft tissue.[32–34]

Key to application of polyester-based materials in biomedicine is optimized surface properties. Surface modification concomitantly results in increased hydrophilicity and the incorporation of new chemical groups onto the surface, which improve the biological response of anchorage-dependent cells. The current study applied different surface modification techniques as outlined in Table I. Base hydrolysis of polyesters can be used as a means to introduce carboxylate groups on the surface[7,35,36] and can subsequently be used to graft functional molecules to or from the surface. Surface modifications can also be achieved by graft copolymerization using

TABLE I. Overview of samples included in the surface layer stability study.

Sample name	Substrate	Surface treatment	Characteristic feature[a]
$PLGA_p$	Particle	None	Size (PDI) = 160 nm (0.12)
h-$PLGA_p$	Particle	Hydrolysis	Size (PDI) = 180 nm (0.32)
$PLGA_f$	Film	None	F/C = 0.02
h-$PLGA_f$	Film	Hydrolysis	F/C = 0.09
PCL_f	Film	None	N/C and S/C = 0
a-PCL_f	Film	Grafting AEMA	N/C = 4.6×10^{-2}
s-PCL_f	Film	Grafting SPA	S/C = 8.8×10^{-3}
PCL_d	Disk	None	N/C and S/C = 0
a-PCL_d	Disk	Grafting AEMA	N/C = 3.8×10^{-2}
s-PCL_d	Disk	Grafting SPA	S/C = 2.0×10^{-2}
h-PCL_s	Scaffold	Hydrolysis	F/C = 0.035
L-PCL_s	Scaffold	Grafting L-lysine(Boc)	N/C = 0.12

[a]The characteristic features of the materials are determined from DLS for the particle samples and reported as the number average particle diameter or from atomic ratios from XPS for the remaining samples.

ionizing radiation to introduce grafted chains with functional groups on the surface.[9,30]

The structure of the substrates and the introduced surface layer potentially play a role in the rate and mechanism of degradation,[14] and an evaluation of such effects is important for the evaluation of their application in biomedicine. In this study, degradation of different surfaces and an evaluation of the effect of the polymer, the chemical modification, and the structure was done for the samples included in Table I. There are three separate components in this study The first component relates to the PLGA materials and the effect of hydrolysis and this is discussed in Sec. III B. The second component discussed in Sec. III C relates to the gamma irradiation-induced grafting of functional monomers to PCL. The third component discussed in Sec. III D relates to hydrolysis and the subsequent grafting of L-lysine to PCL scaffolds. Some characterization of the substrates before and after surface modification is included in the sections below as they serve as control samples. In addition, further characterization of the materials has been included (Figs. S1–S8 in the supplementary material).[54]

B. Surface layer stability evaluation for $PLGA_f$ (film)- and $PLGA_p$ (particle)-based materials

PLGA substrates included spun-coated films ($PLGA_f$) with an initial thickness of 33 ± 2 nm (Fig. S3 in the supplementary material)[54] and particles ($PLGA_p$) with an initial size of 160 nm. These materials underwent base hydrolysis (forming h-$PLGA_f$ and h-$PLGA_p$). Figure 1 shows the comparison between the erosion of thin films (1a) and particle systems (1b) with and without the surface modification process. The erosion of the h-$PLGA_p$ samples was evaluated in PBS, while the $PLGA_p$ sample was evaluated both in PBS and in water.

Modification of $PLGA_f$ by base hydrolysis reduced the film thickness by 15 ± 1 nm before PBS immersion where the total erosion of the sample, h-$PLGA_f$, was determined to be 17 ± 1 nm, in comparison with 33 ± 2 nm for $PLGA_f$. From Fig. 1(a), it can be seen that in both cases, significant erosion did not occur within one day of immersion in PBS, but this was observed within 3 days ($p < 0.05$). At day 14, $PLGA_f$ and h-$PLGA_f$ had eroded by 30 nm (100%) and 3 nm (13%), respectively. The average rate of erosion was approximately 10 times greater for $PLGA_f$ than that for h-$PLGA_f$ at 2.1 ± 0.2 nm/day and 0.23 ± 0.06 nm/day, respectively, over 14 days.

For the particles, base hydrolysis did not cause a significant increase in the number mean particle size or PDI, and in both cases, the apparent change was due to an increase in the skewness of the particle size distribution (Fig. S1 in the supplementary material).[54] The value for the initial size was 160 ± 10 nm for $PLGA_p$ in both water and in PBS and 180 ± 20 nm for h-$PLGA_p$ in PBS. The base hydrolysis of $PLGA_p$ caused an increase in the PDI based on the intensity particle size from 0.15 ± 0.02 to 0.32 ± 0.03 where a bimodal distribution was observed in duplicate samples (Fig. S2 in the supplementary material).[54] As displayed in Fig. 1(b), after 14 days in PBS, the particle sizes of $PLGA_p$ and h-$PLGA_p$ reduced by 33 ± 6 nm and 25 ± 8 nm, respectively. A significant change in the particle sizes was observed after 7 days ($PLGA_p$ $p < 0.0005$ and h-$PLGA_p$ $p < 0.0001$) with no change after that time point. $PLGA_p$ in water initially increased in size by 17 ± 4 nm at day 3 and then reduced in size by 24 ± 5 nm after an additional 18 days. As shown in Fig. 1(c), the PDI of each sample reduced initially until day 3 followed by a statistically significant increase ($p < 0.05$) of 0.05 ± 0.01 and 0.07 ± 0.01 for $PLGA_p$ and h-$PLGA_p$, respectively, between day 3 and 7 when immersed in PBS. Recent work has shown that PLGA particles of low M_w (18 kg mol^{-1}) emulsified with PVA maintained more than 50% of their mass up to 3 weeks in PBS.[37]

Similar research involving PLGA (85:15, L:G) thin films revealed a 10 nm reduction in film thickness after treatment with 50 mM NaOH for 1 h.[38] The current study treated $PLGA_f$ (50:50) with 2.5 mM NaOH for 3 h and observed a 15 nm decrease. This increased erosion can be attributed to decreased hydrophobicity and an increased treatment time of $PLGA_f$ due to an increased net diffusion of solution into the bulk material as the first step of erosion. Oligomer diffusion from the surface and into aqueous

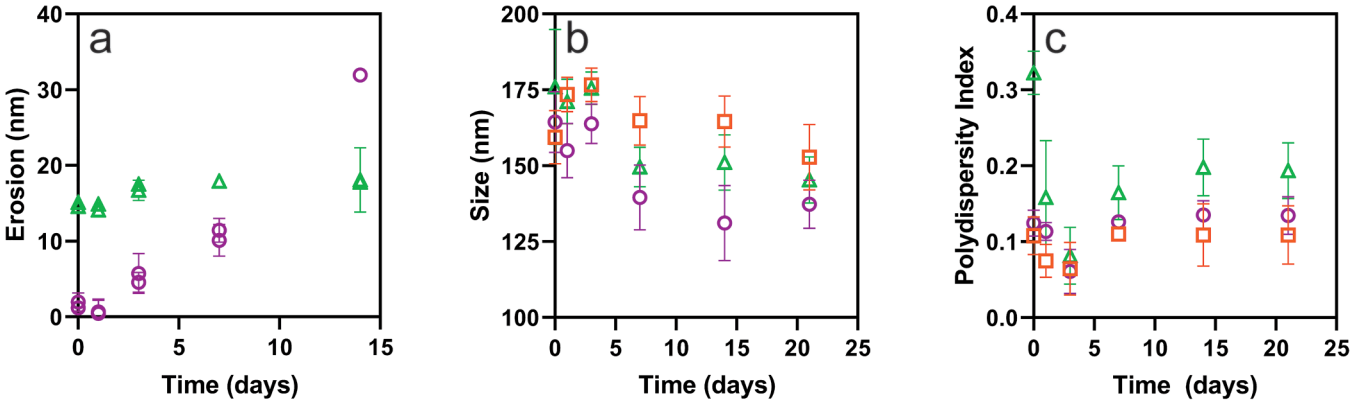

FIG. 1. (a) Erosion (nm) of $PLGA_f$ (○) and h-$PLGA_f$ (Δ) after immersion in PBS for up to 14 days (n = 5 for each replicate). (b) Number average particle size (nm) and (c) PDI of $PLGA_p$ in PBS (○), water (□) and h-$PLGA_p$ in PBS (Δ) over 21 days as measured by DLS (n = 3 for each replicate).

medium is known to occur for PLGA (50:50) oligomers when M_w is less than 630 g mol^{-1} (Ref. 39), and this can account for the observed reduction in film thickness.

When comparing the changes caused by the base hydrolysis of the $PLGA_f$ and $PLGA_p$ samples, a number of factors need to be considered. For the particles, a complex interplay exists between solution uptake and oligomer diffusion as they are coated in PVA, whereas the films are bare. A PVA coating is a physical barrier that minimizes the zeta potential and decreases the hydrophobicity of PLGA particle surfaces.[40] Synergistically, the presence of a PVA coating and a larger surface-to-volume ratio of particles compared to the films likely resulted in an increased PBS uptake. However, PLGA oligomer diffusion out of the particles may have been limited by the PVA barrier as evidenced by the delayed erosion at day 7 for the particles compared to 3 days for the films. Another important distinction between films and particles is the difference between dry and aqueous characterization as the extent of bulk degradation may not be accurately characterized through a measurement of the hydrodynamic size.

Figure 2 shows chemical and morphological changes on the surfaces of the $PLGA_f$ and h-$PLGA_f$ samples. As discussed above, erosion of these materials is caused by hydrolysis as illustrated in Fig. 2(a). The Si/C atomic ratios of the samples as prepared and after immersion in PBS are displayed in Fig. 2(b), with the theoretical value of 1.9 for the silanized silicon wafers indicated. The Si/C atomic ratio of h-$PLGA_f$ was determined to be 0.9 ± 0.1, while for $PLGA_f$, a large spread between duplicates was observed after 14 days of immersion. In both cases, this is a significant increase from <0.01 at the 7-day time point. The value of 1.9 observed after 14 days of immersion in one $PLGA_f$ sample correlates with the polymer film erosion illustrated in Fig. 1(a). Figure 2(c) reports fluorine atom percentage as a relative measure of the carboxylic acid group density on the surface. Silanized wafers functionalized with PFP served as a control with the recorded F 1s At. % of 0.76 indicated in the figure. The relative carboxylic acid density on the surface of $PLGA_f$ immersed in PBS remained constant over the 14-day period. Considering that the F 1s At. % for all samples is close to the value for the control silicon wafer, no conclusion regarding the introduction of carboxylic end groups can be deduced from these data. Base hydrolysis to produce h-$PLGA_f$ caused the introduction of carboxylic acid end groups on the surface with a F 1s At. % of 3.5 ± 0.3%, and this further increased by 1.6 ± 0.3% after PBS immersion for 3 days after which the carboxylic acid density remained constant up to 14 days of immersion. The increase in carboxylic acid density upon the immersion of h-$PLGA_f$ in PBS can be attributed to additional hydrolysis.

The AFM analysis of $PLGA_f$ depicted in Figs. 2(d)–2(g) illustrates the morphological changes upon immersion in PBS over a 7-day period. The measured roughness (R_a) was determined to be 0.15, 7.3, 16, and 7.6 nm after PBS immersion for 0, 1, 3, and 7 days, respectively. The as-prepared $PLGA_f$ sample displays a very smooth morphology that changed to a distorted wave pattern upon immersion in PBS for 1 day. After 3 days of immersion in PBS, craterous surface features were observed, with the diameters ranging from 220 nm to 1.4 μm which developed into larger features resembling rounded stars, with diameters ranging from 3.2 to 4.2 μm at 7 days. At this time point, there was visual evidence of complete polymer erosion in the localized domains which supports the presence of elemental silicon through XPS.

Base hydrolysis to form h-$PLGA_f$ samples resulted in a surface with circular pores with diameters ranging from 100 to 460 nm as shown in Fig. 2(h). Subsequent immersion in PBS [Figs. 2(i)–2(k)] changed the average roughness of the surface to 5.7, 3.8, and 8.2 nm after 1, 3, and 7 days, respectively. After 1 day, localized morphological changes around the circumference of the pores were observed. To quantify this, the average roughness of a 1 μm^2 area localized around the pores was measured to increase from 5.1 nm to 7.7 nm ($p < 0.001$, $n = 5$). This increase in roughness of 2.6 nm localized around the circumference of the pores is attributed to the base prehydrolysis causing an increase in localized carobsylate density and increased local erosion. At day 3, the pore size for the h-$PLGA_f$ sample ranged from 300 to 480 nm, and after 7 days of immersion, the pores developed into craters with sizes ranging from 720 nm to 1.3 μm. A comparison of the crater diameters for $PLGA_f$ and h-$PLGA_f$ after 7 days of PBS immersion [Figs. 2(g) and 2(k)] showed that larger craters formed for the $PLGA_f$ sample, and they were approximately double that of the h-$PLGA_f$ sample. However, an important observation and distinction between the origins of features is observed in $PLGA_f$ and h-$PLGA_f$.

Previous work has described wrinkles and folds forming in polymeric thin films to relieve strain caused by thermal, mechanical, or osmotic stress. Wrinkled arrays observed in Figs. 2(e) and 2(i) are commonly seen in soft polymers with low T_g values (<50 °C) to relieve osmotic stress such as polydimethylsiloxane,[41–43] poly(hydroxyethyl methacrylate),[44] and plasma polymers of monomers tetrahydrofurfuryl methacrylate and 1,2,4-trivinylcyclohexane.[45] $PLGA_f$ and h-$PLGA_f$ ($T_g = 42$–44 °C) may have formed wrinkled arrays likely after swelling in PBS at 37 °C to relieve osmotic and thermal stress. Additionally, the wavelength of wrinkles has been shown to decrease linearly with film thickness resulting in narrower wrinkles which are also observed for h-$PLGA_f$ [Fig. 2(i)].[44]

After immersion for 1 day, $PLGA_f$ was imaged with the data displayed in Fig. 3(a) where distinctly different features can be observed: small pores (square) and early evidence of craters (circled). This suggests that the craterous features observed in Fig. 2(f) for $PLGA_f$ are likely due to the dewetting of polymer films on the silanized wafers when the annealing temperature is higher than the T_g. It has previously been proposed that dewetting can occur through heterogenous nucleation from surface defects or spinodal dewetting.[46,47] It is possible that the features in Figs. 2(g) and 2(k) originate from the two different processes: spinodal dewetting dominating for the $PLGA_f$ sample (shown by a circle) and heterogeneous nucleation dominating for the h-$PLGA_f$ sample (shown by a square). The craters of $PLGA_f$ increase in size after 3 days [Fig. 2(f)] as the polymeric material coalesces at the rim and exposes the underlying silanized wafer at the base of the crater.[38] The contrast between the polymer and the underlying silicon at the rim and base of the crater can be seen in the amplitude [Fig. 3(b)] and phase [Fig. 3(c)] images obtained for $PLGA_f$ imaged under aqueous conditions after immersion in PBS for 3 days. From 3 to 7 days, the craters increase further in size until they

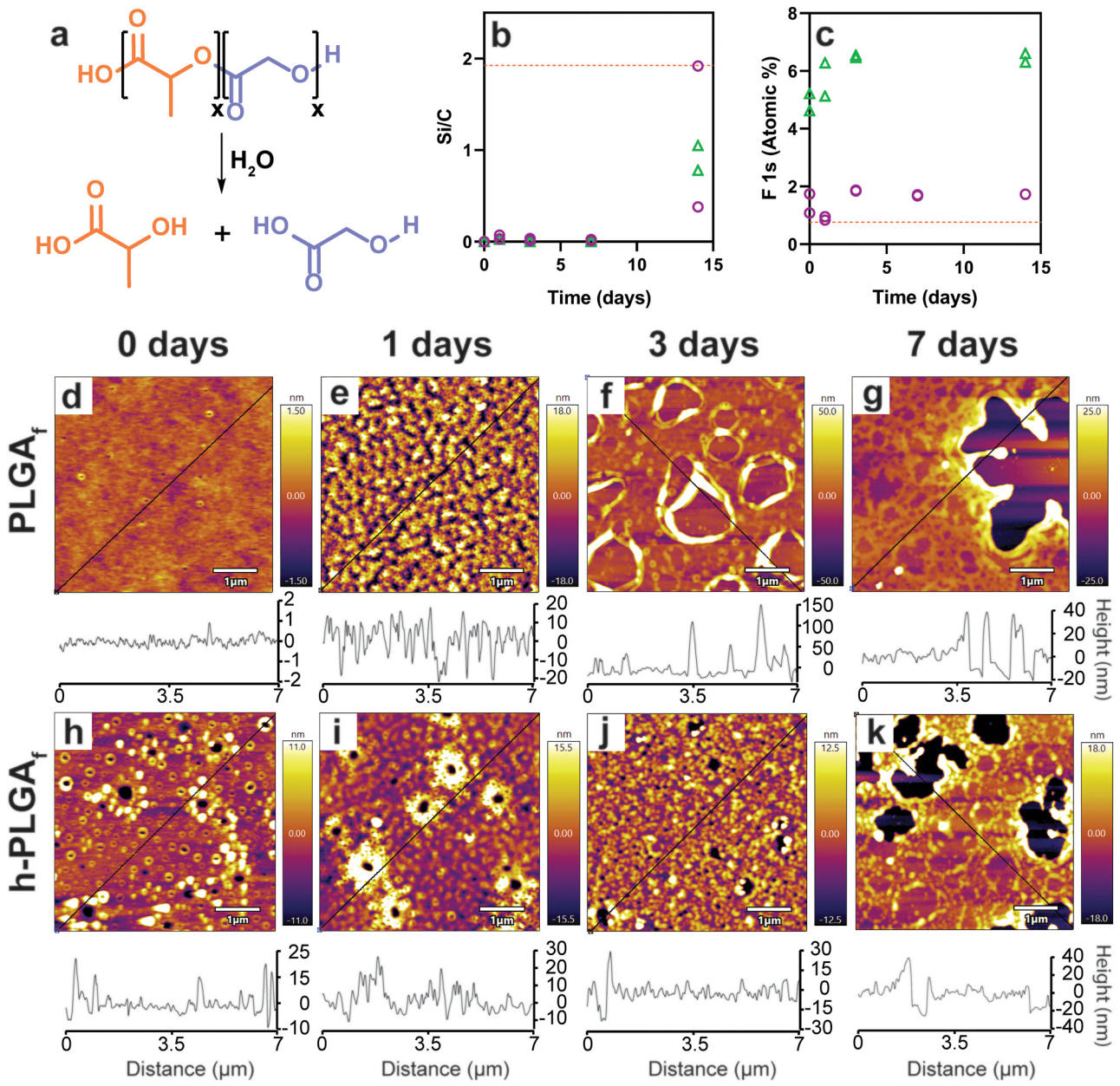

FIG. 2. (a) Reaction scheme for the hydrolysis of PLGA to form lactide and glycolic acid groups. (b) Si 2p/C 1s At. % calculated from XPS survey scans of $PLGA_f$ (○) and h-$PLGA_f$ (△) after PBS immersion for up to 21 days. A TMCS-treated silicon wafer is shown at Si/C = 1.9 as a control (—). (c) The F 1s At. % after film functionalization with PFP as a relative indicator of surface carboxylate density after immersion in PBS for up to 21 days. A PFP-treated TMCS silicon wafer is shown at F 1s At. % = 0.76 as a control. AFM images of $PLGA_f$ [(d)–(g)] and h-$PLGA_f$ [(h)–(k)] at time points 0 [(d) and (h)], 1 [(e) and (i)], 3 [(f) and (j)], and 7 days [(g) and (k)] in PBS. Height traces were drawn diagonally across each sample with the trace represented below each image.

impinge on adjacent craters, forming large-rounded stars seen in Fig. 2(g). Conversely, the pores seen in h-$PLGA_f$ [Fig. 2(h)] are likely caused by hydrolysis at the heterogeneous nucleation sites where defects in the surface increase localized base hydrolysis. After immersion in PBS at 37 °C, the polymer begins to dewet, forming craters originating from the base hydrolysis-induced pores as imaged throughout the lifetime of h-$PLGA_f$ [Figs. 2(h)–2(k)].

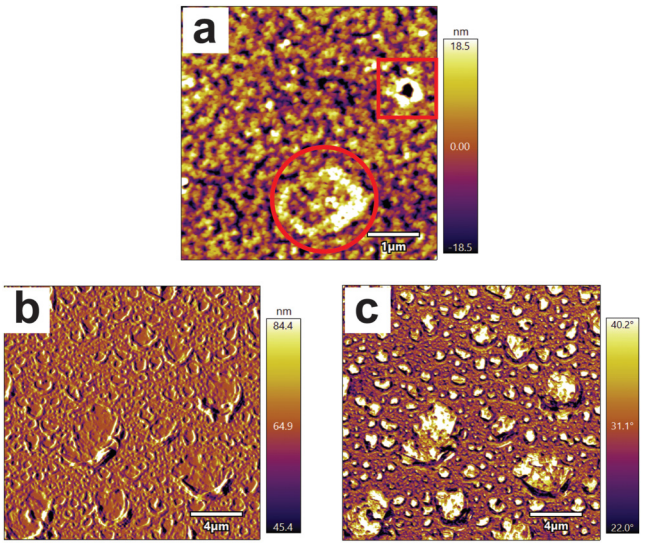

FIG. 3. (a) AFM (ambient conditions) image of $PLGA_f$ at day 1 illustrating two types of pores. Aqueous AFM images of $PLGA_f$ after PBS immersion for 3 days are shown in both the amplitude (b) and phase (c) contrasted images.

C. Surface layer stability evaluation for PCL_f (film)- and PCL_d (disk)-based materials

PCL substrates (PCL_f and PCL_d) were modified with the grafting of AEMA (a-PCL_f and a-PCL_d) or SPA (s-PCL_f and s-PCL_d) monomers by gamma irradiation-induced grafting which is a grafting from processes. The introduction of amine groups can be used to further modify a material with carboxylic acid-containing biomolecules,[12] while sulfonate groups can be effective for electrostatic binding of high p*I* proteins such as growth factors.[48] The modified substrates and unmodified PCL_f and PCL_d were immersed in PBS for up to 21 days. The untreated and modified substrates were analyzed by CA, XPS, AFM, and SEM to assess changes in surface chemistry and morphology as a result of the immersion process.

For the untreated spun-coated film, PCL_f, upon immersion in PBS, the CA values [Fig. 4(a)] decrease from day 7 to day 10 from 74° to 68°, with a significant increase to 75° ($p < 0.0001$) at the 21-day time point. The C/O ratio [Fig. 4(b)], however, is unchanged for the 21-day period and matches the theoretical ratio of 3.0 for PCL. The increase in CA for PCL_f at 21 days may be due to the degradation of the surface causing an increase in roughness. The R_a values obtained from AFM data [Fig. 4(h)] indicate an increase in roughness after immersion in PBS for 21 days. For the untreated melt-pressed disk, PCL_d, the CA values [Fig. 4(d)] show an initial decrease from 80° prior to immersion to 66° after immersion in PBS ($p < 0.0001$) with no significant effect on the immersion time. This trend is mirrored in the C/O ratio [Fig. 4(e)] which displays an initial decrease from 3.3 prior to immersion to 2.8–3.0 after immersion in PBS. The relatively high value for the CA and C/O atomic ratio of PCL_d prior to immersion in PBS could be related to surface contamination. The C 1s carbon narrow scan [Fig. S6(d) in the supplementary material][54] revealed that this substrate had a ratio of 4.1 for C–C to C–O which is higher than the theoretical value of 3.1. For the samples that had been immersed in PBS, there is a consistent trend of the CA value of the PCL_d sample being lower than that of the PCL_f sample, typically 4°–6° lower, with the largest difference at 21 days being 9°. This can be related to the different morphologies of the samples, with the PCL_f sample showing spherulites of approximately 5–10 μm and an R_a value of 2.96 nm, while the PCL_d sample displaying no distinct "spherulite" on this size scale and an R_a value of 12.20 nm [Fig. S5(c) in the supplementary material].[54]

Modification of PCL by gamma irradiation-induced grafting with AEMA as the monomer to form a-PCL was evaluated in regard to the extent of modification using the N/C atomic ratio [Fig. 4(c)]. The a-PCL_f sample displayed a value of 0.046, corresponding to about 3.4% nitrogen in the XPS survey scans, which can be compared to the theoretical N/C atomic ratio of 0.167 (11.1% nitrogen) for poly-AEMA (PAEMA), indicating that these samples have approximately 28% of the XPS signal coming from PAEMA. Similarly, for the a-PCL_d sample [Fig. 4(f)], the N/C atomic ratio was 0.038 corresponding to about 23% of the XPS signal. Thus, there does not appear to be any significant difference in the grafting outcome for these two substrates. A previous study grafting AEMA onto spin-coated PCL films observed a similar N/C atomic ratio of 0.028.[30] For the a-PCL_f samples immersed in PBS, the N/C atomic ratio [Fig. 4(c)] remained constant for the 21-day incubation period. For a-PCL_d [Fig. 4(f)], however, the decrease in the N/C atomic ratio from the initial value of 0.04 to 0.022 after 21 days of incubation in PBS is considered significant.

The CA of a-PCL_f [Fig. 4(a)] was initially higher than that of PCL_f ($p < 0.001$), but after immersion, the CA decreased and was significantly lower compared to PCL_f by 7 to 16° ($p < 0.0001$). A similar observation was made for the a-PCL_d sample where the CA initially was higher than that for a-PCL_f, but after immersion, their values were similar. This decrease in the CA can be explained based on chain rearrangement upon immersion in PBS where the hydrophilic domains (e.g., amine groups) become exposed to the outmost surface, causing a reduction in CA. Both the PCL_f and a-PCL_f samples display an increase in CA at the 21-day time point ($p < 0.0001$). As for the PCL_f sample, this observation of a-PCL_f can be attributed to an increase in surface roughness [Fig. 4(h)].

The C/O atomic ratio [Fig. 4(b)] of the a-PCL_f samples before immersion and during 14 days of immersion in PBS remained unchanged with a value of approximately 3.0, which is the same as the theoretical ratio for both PCL and PAEMA. At the 21-day time point, the C/O atomic ratio for a-PCL_f was reduced from 2.4 to 2.7. One potential explanation would be the hydrolysis of PAEMA yielding poly(methacrylic acid) (PMAAc) and 2-aminoethanol as illustrated in Fig. 4(g) as the theoretical C/O atomic ratio of PMAAc is 2.0. However, there is no corresponding decrease in the N/C ratio, making this explanation less plausible. In the case of the a-PCL_d samples [Fig. 4(e)], the change in the C/O atomic ratio is very similar to that observed for the a-PCL_f samples, with a similar decrease after 21 days. In this case, however, it is paralleled by a decrease in the N/C atomic ratio. Another cause of the observed decrease in the C/O atomic ratio could be the hydrolysis of the PCL substrate as the theoretical C/O atomic ratio of 100% hydrolyzed

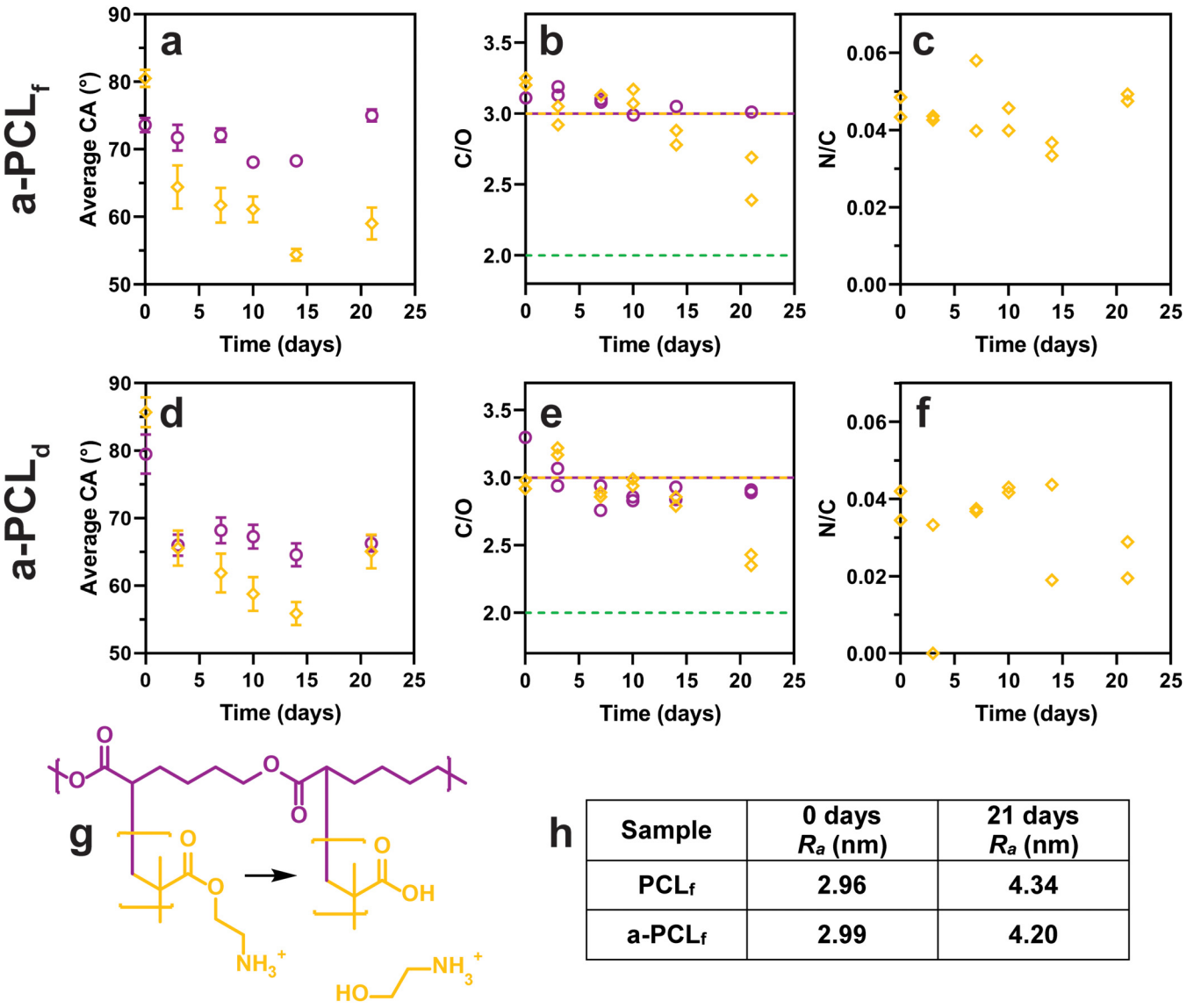

Sample	0 days R_a (nm)	21 days R_a (nm)
PCL$_f$	2.96	4.34
a-PCL$_f$	2.99	4.20

FIG. 4. Surface analysis of PCL (○) and a-PCL (◇) samples. (a)–(c) PCL$_f$ and a-PCL$_f$, (d)–(f) PCL$_d$ and a-PCL$_d$. (a) and (d) CA represented as average ± SD, n = 16, except for PCL$_f$ 10–21 days ($6 \leq n \leq 8$). (b) and (e) XPS C/O atomic ratio, (purple line) theoretical PCL ratio = 3.0, (yellow line) theoretical PAEMA ratio = 3.0, (—) theoretical hydrolyzed PAEMA ratio = 2.0. (c) and (f) XPS N/C atomic ratio. (g) Diagram of PAEMA hydrolysis. (h) Table of AFM roughness (R_a) values calculated (see Fig. 6 for AFM micrographs).

PCL is 2.0. However, neither the formation of PMAAc nor the hydrolysis of the PCL substrate is in agreement with the increase in CA as the carboxylate groups introduced by these processes would be expected to be more hydrophilic than the amine groups.

Modification of PCL by gamma irradiation-induced grafting with SPA as the monomer to form s-PCL substrates can be evaluated from the S/C atomic ratio. For s-PCL$_f$, the S/C atomic ratio [Fig. 5(c)] is between 0.006 and 0.012. Considering that pure poly-SPA (PSPA) has a theoretical S/C atomic ratio of 0.167 (8.3% sulfur), these samples have approximately 5% of the XPS signal due to PSPA. For the s-PCL$_d$ sample [Fig. 5(f)], an initial S/C atomic ratio of 0.02 corresponds to approximately 12% of the XPS signal being from PSPA. This is a significantly higher degree of surface modification, yet, for both samples, the degree of grafting is low and the sulfur content rapidly decreases after PBS immersion. In many samples after immersion, no sulfur is detected, suggesting that the surface layer is lost within the first few days in PBS.

The CA for s-PCL$_f$ [Fig. 5(a)] is initially lower than that for PCL$_f$ by 4.5° ($p < 0.0001$) in accordance with successful grafting. The C/O atomic ratio of s-PCL$_f$ [Fig. 5(b)] is lower than that of

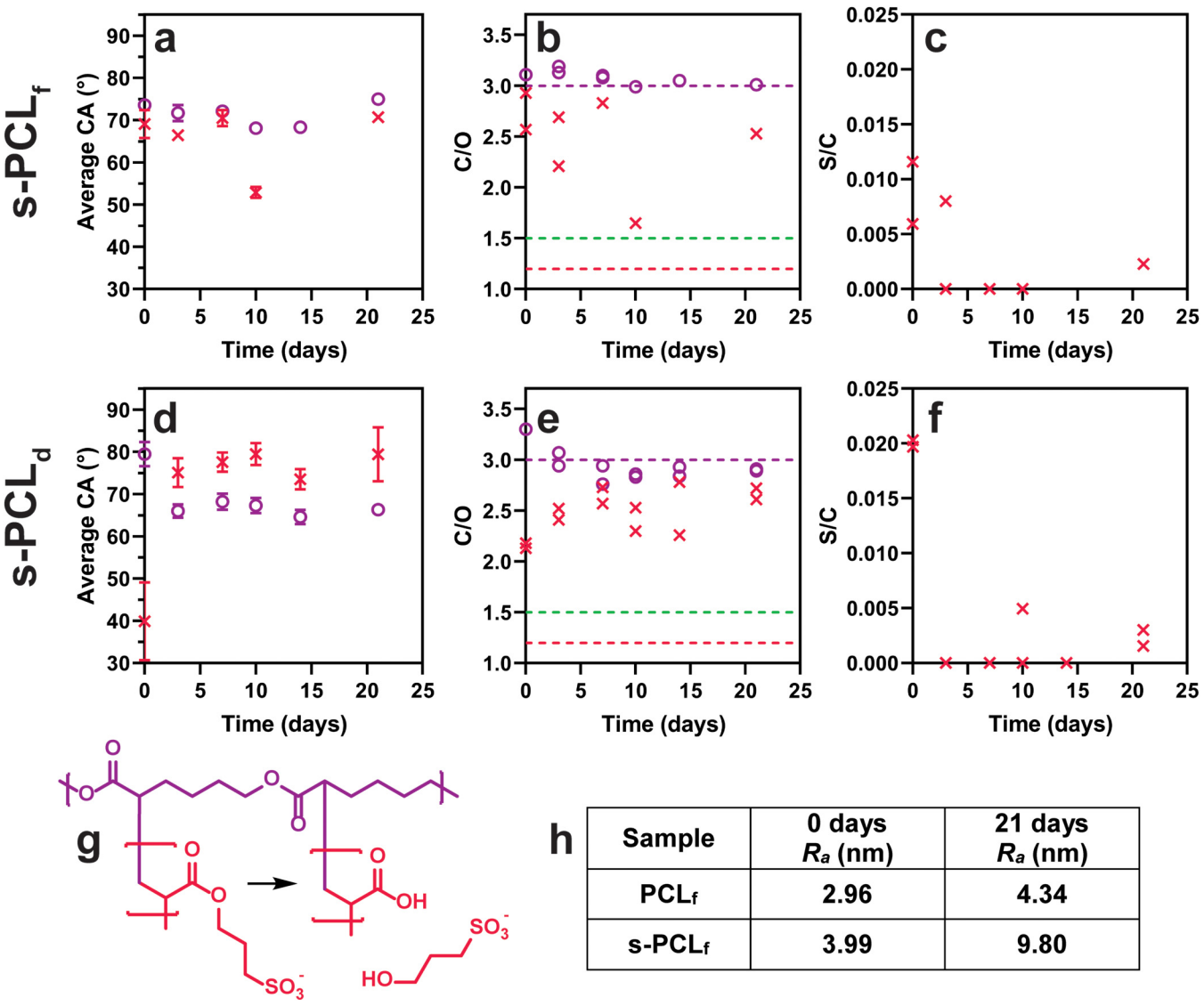

Sample	0 days R_a (nm)	21 days R_a (nm)
PCL$_f$	2.96	4.34
s-PCL$_f$	3.99	9.80

FIG. 5. Surface analysis of PCL (○) and s-PCL (×) samples. (a)–(c) PCL$_f$ and s-PCL$_f$, (d)–(f) PCL$_d$ and s-PCL$_d$. (a) and (d) CA represented as average ± SD, n = 16, except for PCL$_f$ 10–21 days and s-PCL$_d$ 10 days ($6 \le n \le 8$), and s-PCL$_f$ 7–21 days ($2 \le n \le 8$). (b) and (e) XPS C/O atomic ratio, (purple line) theoretical PCL ratio = 3.0, (red line) theoretical PSPA ratio = 1.2, and (green line) theoretical hydrolyzed PSPA ratio = 1.5. (c) and (f) XPS S/C atomic ratio. (g) Diagram of PSPA hydrolysis. (h) Table of AFM roughness (R_a) values calculated (see Fig. 6 for AFM micrographs). The PCL$_f$ and PCL$_d$ data (○) from Fig. 4 have been included in Fig. 5 for comparison with s-PCL samples (×).

unmodified PCL$_f$ in agreement with the theoretical C/O atomic ratio of PSPA being 1.2 and therefore also supports successful grafting. For the s-PCL$_d$ sample, the significant reduction in CA (to 40°, $P < 0.0001$) and in the C/O atomic ratio (to 2.1) relative to unmodified PCL$_d$ is more pronounced than that for the PCL$_f$ samples which is in agreement with the S/C atomic ratios observed. The surface layer stability was evaluated from the CA values and C/O atomic ratios. For the s-PCL$_f$ sample, the CA is similar to that of PCL$_f$ over the 21-day period, except for the 10-day time point (which appears to be an outlier). Likewise, there is no clear indication from the C/O atomic ratio that any change is taking place (the 10-day time point again being an outlier). The reason for this could be either the surface layer is stable for the 21-day period of the study or indeed the surface layer is lost very early during immersion in PBS.

A more complete data set can be found for the PCL$_d$ samples with CA and C/O atomic ratios depicted in Figs. 5(d) and 5(e). After immersion of s-PCL$_d$ in PBS, the CA increases significantly

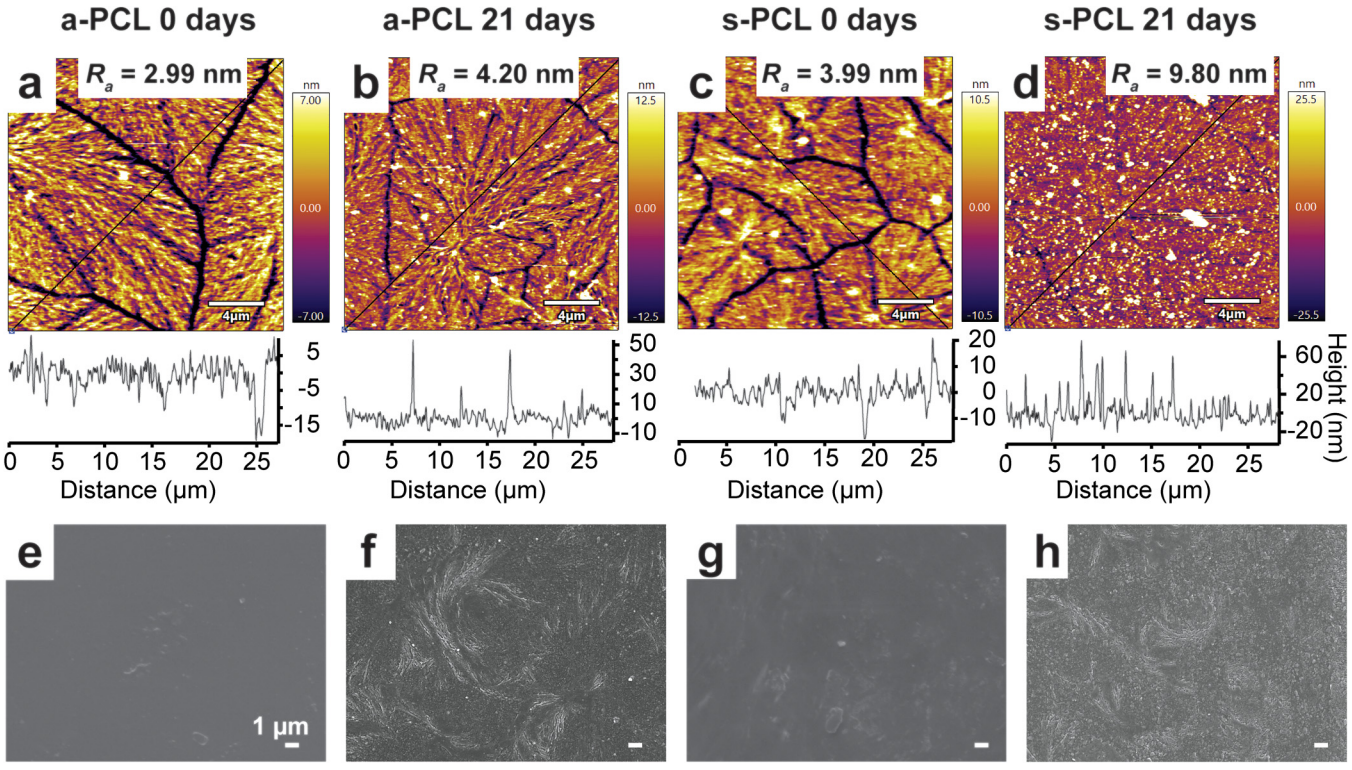

FIG. 6. Surface morphological analysis of a-PCL samples [(a), (b), (e), and (f)] and s-PCL samples [(c), (d), (g), and (h)]. AFM micrographs and height traces of (a) a-PCL_f 0 days, (b) a-PCL_f 21 days, (c) s-PCL_f 0 days, and (d) s-PCL_f 21 days. Roughness (R_a) values have been calculated for the entire regions and height traces have been taken along the diagonal highlighted by the black lines. SEM micrographs of (e) a-PCL_d 0 days, (f) a-PCL_d 21 days, (g) s-PCL_d 0 days, and (h) s-PCL_d 21 days.

compared to that of the as-prepared sample to a value that is significantly higher than that of unmodified PCL_d. There is no significant change in the CA value with immersion time for the 21-day time period. The C/O atomic ratio displays a general increase with time for s-PCL_d toward the theoretical value of PCL. There is no evidence for any of the samples grafted with SPA that hydrolysis of the grafted PSPA chains to form poly(acrylic acid) (PAAc) and 3-hydroxypropane sulfonate [Fig. 5(g)] is occurring. As pointed out for the s-PCL_f sample, it is most likely that the grafted chains are removed rapidly after immersion in PBS.

The crystalline domain boundaries of the modified PCL_f samples can be observed in the AFM micrographs [Figs. 6(a)–6(d)]. After grafting with AEMA, the R_a of the entire image of PCL_f [Figs. S5(a) in the supplementary material and Figs. 6(a) and 6(c)][54] remains similar, changing from 2.96 to 2.99 nm, and increases to 3.99 nm after grafting with SPA. Similar observations have previously been made for the grafting of AEMA and AAc to PCL spun-coated films.[30] After grafting, the widths of the crystalline domain boundaries are similar to unmodified PCL_f but decrease after PBS immersion for 21 days [Figs. 6(b) and 6(d)]. For the s-PCL_f sample measured after 21 days, the boundaries are almost indistinguishable from the rest of the film. While this is different from that of the control PCL_f sample, it is possible that the gamma irradiation process has caused these changes. The R_a values of the grafted PCL_f samples increase after PBS immersion for 21 days to 4.20 nm for a-PCL_f and 9.80 nm for s-PCL_f. For a-PCL_f, this correlates with the increase in CA; however, this same increase is not observed for the s-PCL_f samples.

For unmodified PCL_d samples [Figs. S5(d) and S5(e) in the supplementary material],[54] there are relatively minor changes in morphology detected by SEM after PBS immersion for 21 days. There is no clear difference in the PCL_d samples after grafting with AEMA or SPA [Figs. 6(e) and 6(g)]. There is, however, a significant change in morphology after immersion of the grafted PCL_d samples [Figs. 6(f) and 6(h)] for 21 days in PBS. While it is shown that the AEMA surface layer remains present for the 21-day incubation period, it is most likely that the SPA surface layer is removed quickly after immersion in PBS. This is an interesting result given that the largest change in surface morphology is seen for the SPA-grafted samples. It would be expected that the hydrophilic surface layer (AEMA or SPA) could increase the rate of surface erosion of a hydrophobic substrate but not so if the surface layer is removed quickly. However, it has previously been shown for the grafting of poly(sodium styrene sulfonate) to PCL that Mohr's salt can cause an excessive degradation of the substrate, resulting in cracks visible by SEM, and a reduction in the M_w of the bulk material.[8] The element

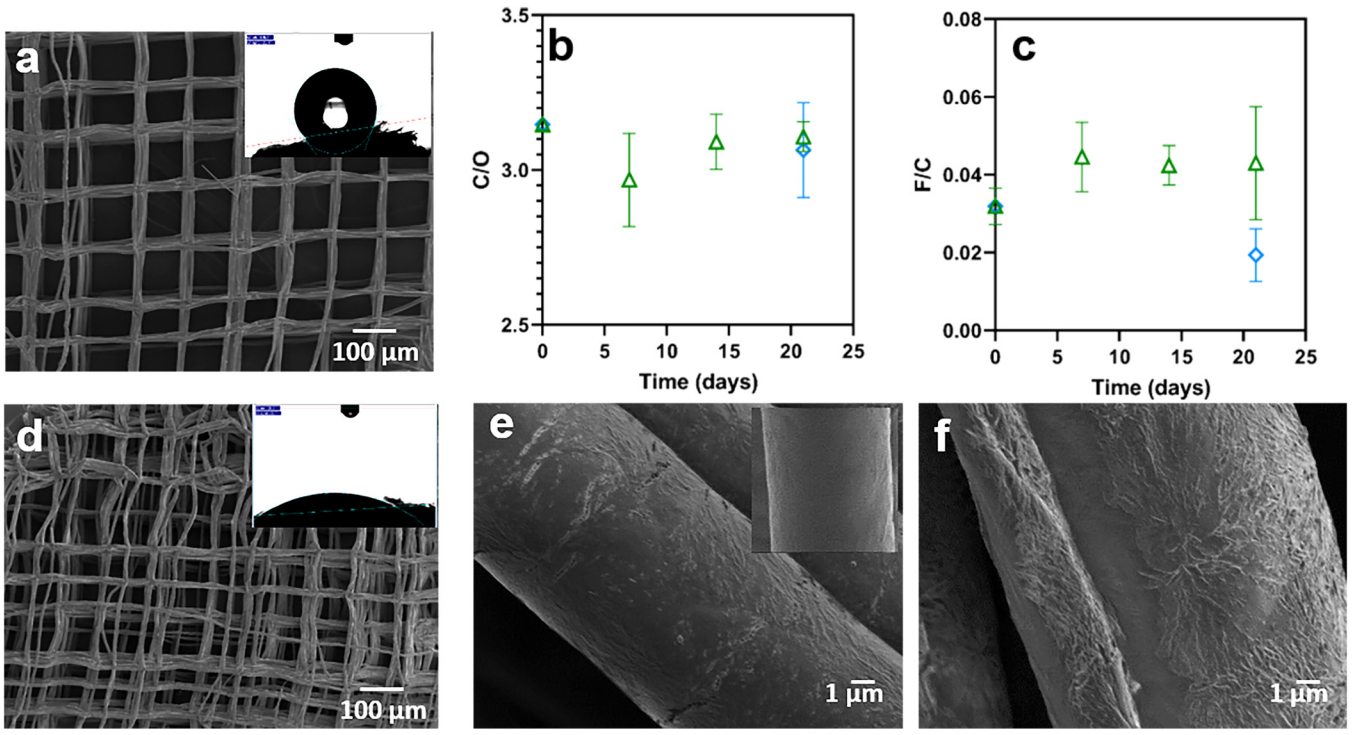

FIG. 7. (a) SEM micrographs and CA of PCL_s. XPS data before and after immersion in PBS (△) and water (◇), (b) C/O atomic ratio of h-PCL_s, (c) F/C atomic ratio of h-PCL_s. The results are shown as average value ± standard deviation n = 3. (d) SEM micrographs and CA of h-PCL_s, (e) SEM of h-PCL_s (inset PCL before hydrolysis), and (f) after 21 days of immersion in PBS.

iron (from Mohr's salt) can be detected by XPS in most SPA-grafted samples up to approximately 1.5 At. %, so the significant change in the surface morphology of the SPA-grafted samples may be contributed by the presence of Mohr's salt, both during the grafting process and during the immersion of the material.

D. Surface layer stability evaluation for PCL_s (scaffold)-based materials

PCL melt-electrowritten scaffolds (PCL_s) were modified by base hydrolysis to obtain h-PCL_s. These samples were grafted with L-lysine(Boc) to produce L-PCL_s. These modified substrates were immersed in PBS for up to 21 days and analyzed by XPS and SEM to evaluate changes in surface chemistry and morphology due to the immersion process.

Figure 7 details the observation made for hydrolysis of the scaffolds. The SEM micrographs show the macroscopic structure of PCL_s [Fig. 7(a)] and h-PCL_s [Fig. 7(d)]. There is a decrease in the alignment of the fibers after the hydrolysis treatment, probably due to the agitation process, which affects the overall scaffold structure, creating some displacement between layers as can be observed in previous studies.[33] CA measurements were in this case used as a qualitative measure of the success of the surface treatment. The insets in Figs. 7(a) and 7(d) show marked differences in the contact angle before (125°) and after (31°) the hydrolysis, confirming the introduction of carboxylate groups on the surface. At a higher magnification of the scaffold fibers displayed in Fig. 7(e), it can be observed that base hydrolysis changes the surface morphology from smooth (PCL_s shown in the inset) to pitted and overall rougher (h-PCL_s) which has been reported previously.[24]

The h-PCL_s samples were immersed in PBS or water for 21 days to evaluate the changes in the surface chemistry and surface morphology. There was no significant change in the C/O atomic ratio [Fig. 7(b)] after 7, 14, and 21 days in PBS or after 21 days in water compared to the value for the as-prepared samples. The C/O atomic ratios for all samples were very similar to that of the theoretical ratio of 3.0 for PCL. The relative carboxylate density was evaluated as described above through treatment with PFP. The F/C atomic ratio [Fig. 7(c)] did not change significantly during immersion in PBS but did show an apparent reduction upon immersion in water. These data indicate that the hydrolyzed surface layer on the h-PCL_s samples was maintained during immersion for 21 days in PBS. SEM micrographs of h-PCL_s immersed in PBS for 21 days [Fig. 7(f)] illustrate that there are no morphological changes during the immersion process.

While h-PCL_s has increased the hydrophilicity, scaffolds that have been further modified with biological molecules have an increased potential for biomedical applications.[49] In this study, L-lysine(Boc) was grafted on the surface after the hydrolysis using

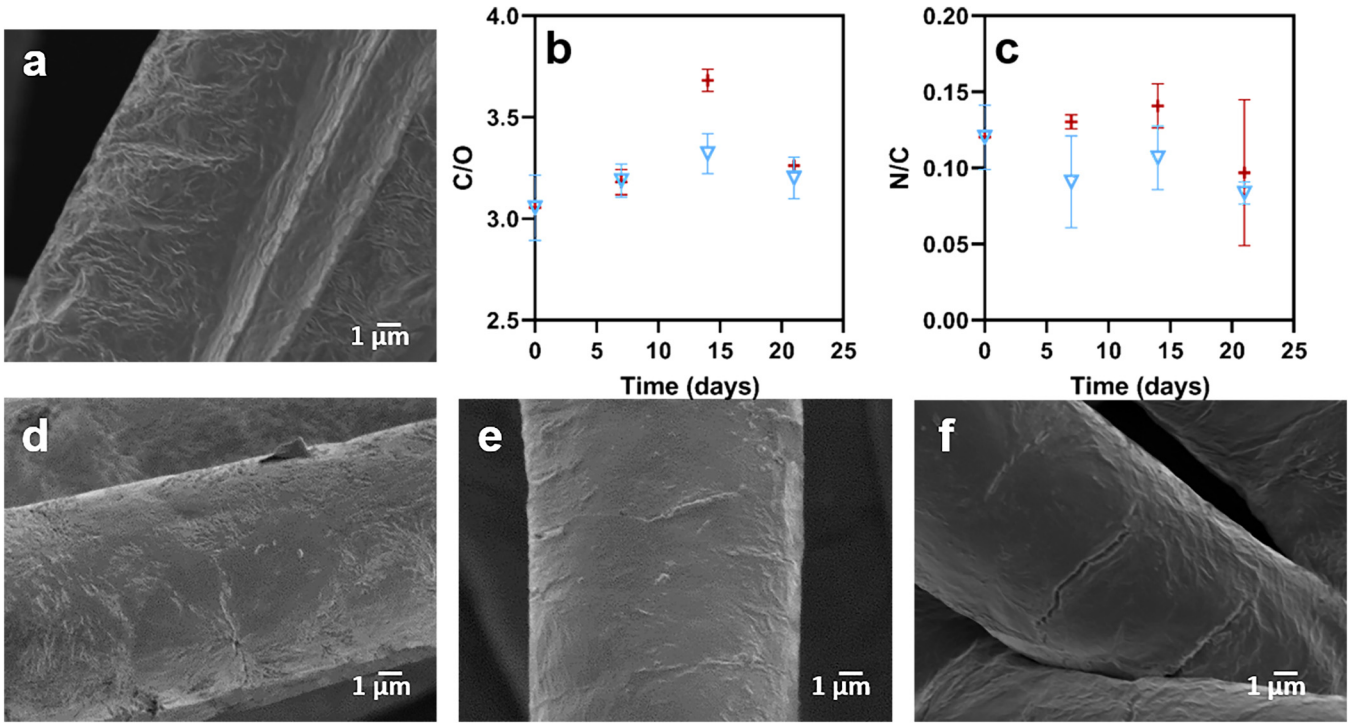

FIG. 8. (a) SEM micrographs of L-PCL$_s$, XPS data (b) C/O atomic ratio of L-PCL$_s$, and (c) F/C atomic ratio of L-PCL$_s$ in (▽) PBS and (+) water; the results are shown as average value ± standard deviation (n = 3). SEM micrographs after L-PCL$_s$ immersion in PBS for (d) 7 days, (e) 14 days, and (f) 21 days.

EDC chemistry. Figure 8(a) shows the surface morphology of a scaffold fiber of L-PCL$_s$ which is similar to that of h-PCL$_s$, indicating that the functionalization process did not affect the surface morphology. The C/O atomic ratio of the samples was 3.15, which is not considered statistically different from that of h-PCL$_s$ (C/O = 3.07). The functionalization with L-lysine(Boc) was achieved using grafting from the surface carboxylate groups and as such can result in the formation of oligomers. The initial F/C atomic ratio is 0.03 for the h-PCLs sample. It is noted that 5 F atoms are introduced per carboxylate group upon functionalization with PFP. In addition, the N/C atomic ratio is 0.12 for the L-PCLs sample, where each L-lysine(Boc) will contribute 2N atoms. Based on this, it can be calculated that oligomers with an average of approximately 10 units are introduced on the surface.

The L-PCL$_s$ samples were immersed in water and in PBS. Figure 8(b) demonstrates that the C/O atomic ratio of the samples shows a similar trend when immersed in water or in PBS, with a significantly higher value for the 14-day time point (which appears to be an outlier). During the immersion process, the N/C atomic ratio displayed in Fig. 8(c) was found to be significantly lower after 21 days of immersion in PBS, while the data obtained from immersion in water did not show any significant change. This indicates that the grafted L-lysine(Boc) is in part eroded from the surface in PBS.

SEM images of the L-PCL$_s$ samples after immersion in PBS for 7, 14, and 21 days [Figs. 8(d)–8(f)] show small cracks on the surface. These cracks were observed in all the samples, being more pronounced after 21 days. In contrast, as shown in Fig. 7(e), the hydrolysis creates random fissures on the surface, which do not increase in size or number during the degradation study. However, the quantification of those defects is very challenging due to their random locations over the scaffold surface. These morphological changes during the degradation study suggest that the hydrolysis and the subsequent grafting affect the surface stability in terms of morphology, accelerating the surface degradation in PBS relative to h-PCL$_s$. It has previously been shown that longer *in vitro* cell studies of 3D printed PCL hydrolyzed scaffolds similarly cause the formation of such cracks without any grafting process.[24] For this reason, longer degradation studies are required to confirm this trend.

IV. SUMMARY AND CONCLUSIONS

Selection of a surface modification strategy must take into account the relative longevity of the surface layer and the bulk material, and an evaluation of such material properties should be a core component when developing surface-modified materials for use in biomedicine. The current study investigated in detail a number of polyester-based substrates that had been subjected to surface modification. A number of important lessons can be drawn from this work.

The use of model substrates is attractive as it allows more detailed analysis of changes in wettability and surface topography.

TABLE II. Overview of longevity of the surface layers based on the current surface layer stability study.

Sample name[a]	Unaltered, lifetime (UL)	Functional, lifetime (FL)	Method of evaluation	Cause of degradation
h-$PLGA_p$	3 days	>21 days	DLS (UL and FL)	Hydrolysis
h-$PLGA_f$	1 day	>14 days	F At. % from XPS (UL) AFM and XPS (FL)	Hydrolysis and de-wetting
a-PCL_f	14 days	>21 days	XPS and CA (UL), C/O ratio from XPS (FL)	Unknown
s-PCL_f	<3 days	<3 days	XPS and CA (UL and FL)	Mohr's salt
a-PCL_d	14 days	>21 days	XPS and CA (UL), C/O ratio from XPS (FL)	Unknown
s-PCL_d	<3 days	<3 days	XPS and CA (UL and FL)	Mohr's salt
h-PCL_s	14 days in water, >21 days in PBS	>21 days	XPS (UL), F/C ratio from XPS (FL)	Hydrolysis
L-PCL_s	>14 days	>21 days	XPS (UL), N/C ratio from XPS (FL)	Unknown

[a]Prefix denotes modification and subscript the substrate, i.e., prehydrolyzed samples are denoted "h-" prefix, AEMA grafted samples are denoted "a-" prefix, SPA grafted samples are denoted "s-" prefix, L-lysine(Boc)-grafted samples are denoted "L-" prefix, particle substrates are given a "p" subscript, film substrates are given "f" subscript, disk substrates are given "d" subscript, and scaffolds are given "s" subscript.

Thin films on silicon wafers or glass slides, for example, are frequently used in this regard.[7,19,25,50–52] However, it is evident from the current work that in many cases this may lead to erroneous interpretations. In the case of the $PLGA_f$-based materials, dewetting due to the underlying silicon wafer was observed. This phenomenon, however, is not relevant to the particle system that it intended to model. For the PCL_f-based materials, delamination caused technical challenges that were not present when the PCL_d-based materials were used. It is, therefore, questionable if the use of model substrates is indeed an overall advantage.

An overview of the findings of the current study in regard to the longevity of the surface layers is summarized in Table II. The lifetime was evaluated using different approaches depending on the type of substrate being evaluated. In some cases, different methods of evaluation lead to different estimations of unaltered and/or functional lifetimes. In such cases, the shortest lifetime is reported. One example is the unaltered lifetime of a-PCL_f samples. The CA data and N/C atomic ratio indicated that the surface is unchanged after immersion for 21 days, and the unaltered lifetime would be >21 days according to these methods. However, the C/O atomic ratio decreases significantly at the 21-day time point, so the reported unaltered lifetime for this sample is 14 days.

Using base hydrolysis to introduce carboxylate groups on PLGA- and PCL-based materials resulted in surface layers of high stability. For example, $PLGA_p$ showed similar solution stability for 21 days regardless of whether they were treated by base hydrolysis or not, and h-PCL_s showed no reduction in carboxylic acid density after immersion for 21 days in PBS, while in water, the unaltered lifetime was shorter. While ester hydrolysis is not governed by the kinetic salt effect, it has been classified as an ion-dipole reaction, and a decrease in the rate constant with an increase in ionic strength has been reported.[53] This is in agreement with the observations in this study. Overall, it can be concluded that despite the reduction in the polymer molecular weight at the surface of the material caused by the prehydrolysis, this modification strategy appears to be sound. This is in contrast to the use of aminolysis as discussed in the Introduction.

The introduction of hydrophilic grafted polymer chains on a hydrophobic surface may increase the rate of hydrolysis of the surface layer by enabling the PBS solution or water to further penetrate into the PCL substrate, a similar observation as that of the grafting front mechanism. Previous studies have observed enhanced water uptake of solvent cast PCL films after grafting with acrylic acid.[9] In the current study, the surface layer stability of grafted layers was evaluated for PCL_f- PCL_d,- and PCL_s-based materials. For the samples produced using gamma irradiation-induced grafting, the requirement for the addition of Mohr's salt when using the monomer SPA caused additional surface damage which led to displacement of the grafted PSPA chains after short-term immersion in PBS, resulting in a lifetime of less than 3 days. In contrast, a PAEMA graft copolymer displayed high stability for 14 days (unaltered lifetime) with evidence of surface layer erosion at day 21. Similarly, the grafting of L-lysine(Boc) from h-PCL_s samples to produce L-PCL_s resulted in a surface layer with high stability for 21 days in PBS and some evidence of erosion at the 21-day time point. It thus appears that such covalently attached surface layers have a finite lifetime that is significantly shorter than that of the bulk material.

A number of the unanswered questions in the sections above could potentially be answered with the use of surface analysis methods that better probe the outmost atomic layer [e.g., angle-resolved XPS or time-of-flight secondary ion mass spectrometry (ToF-SIMS)]. Additional molecular information gained from ToF-SIMS may also be able to give further insight into degradation mechanisms. This is the case for evaluating the distribution and thereby the formation of carboxylic end groups in $PLGA_f$ substrates during the degradation process and for gaining a more detailed understanding of the mechanism of degradation of PCL-based materials with grafted chains. For example, is the entire grafted chain displaced from the surface or is the loss of nitrogen observed by XPS due to hydrolysis within the grafted chains? Furthermore, for analysis of nano-sized particles, additional measurement of particle concentration (e.g., using nanoparticle tracking analysis) could potentially better reflect the degradation process.

The current study has demonstrated that hydrolysis appears to be a viable method for modification of PLGA particles with intended

use for cancer therapy where an improved circulation half-life is required for these types of systems to be effective.[5] Evaluation of serum stability would be required prior to further development. Furthermore, the use of PCL-based scaffolds with grafted chains (e.g., PAEMA or L-lysine(Boc)) may indeed have the required lifetime to allow tissue interaction. The use of SPA as the monomer for gamma irradiation-induced grafting, or indeed as other monomers that require the presence of homopolymer inhibitors, would appear not to be a viable option. This work thus demonstrates the importance of evaluating the chemical and morphological changes and the lifetime of the surface layer in solution at physiological *p*H and temperature. This allows an initial screening of a surface modification approach. When designing materials for use in biomedicine, further evaluation of protein adsorption and cellular interactions, for example, is required to establish their impact on the stability of the surface layers.

AUTHORS' CONTRIBUTIONS

H.P. and A.L.M. contributed equally to this work.

ACKNOWLEDGMENTS

D.G.C. gratefully acknowledges support from United States National Institutes of Health Grant No. EB-002027. A.A. is thankful to the National Health and Medical Research Council, Australia, for the Early Career Research Fellowship (Nos. APP1123340 and 2017–2021) for providing financial support. H.P. and A.L.M. acknowledge Australian Government RTP scholarship Funding. The authors acknowledge the facilities and the scientific and technical assistance of the Australian Microscopy & Microanalysis Research Facility at the Centre for Microscopy and Microanalysis, The University of Queensland. This work was performed in part at the Queensland node of the Australian National Fabrication Facility, a company established under the National Collaborative Research Infrastructure Strategy to provide nano- and microfabrication facilities for Australia's researchers.

DATA AVAILABILITY

The data that support the findings of this study are available from the corresponding author upon reasonable request.

REFERENCES

[1]M. Bartnikowski, T. R. Dargaville, S. Ivanovski, and D. W. Hutmacher, Prog. Polym. Sci. **96**, 1 (2019).
[2]C. Martins, F. Sousa, F. Araújo, and B. Sarmento, Adv. Healthcare Mater. **7**, 1701035 (2018).
[3]I. Manavitehrani, A. Fathi, H. Badr, S. Daly, A. N. Shirazi, and F. Dehghani, Polymers **8**, 20 (2016).
[4]L. N. Woodard and M. A. Grunlan, ACS Macro Lett. **7**, 976 (2018).
[5]E. M. Elmowafy, M. Tiboni, and M. E. Soliman, *Biocompatibility, Biodegradation and Biomedical Applications of Poly (Lactic Acid)/ Poly (Lactic-co-Glycolic Acid) Micro and Nanoparticles* (Springer, Singapore, 2019).
[6]L. Grøndahl, A. Chandler-Temple, and M. Trau, Biomacromolecules **6**, 2197 (2005).
[7]T. I. Croll, A. J. O'Connor, G. W. Stevens, and J. J. Cooper-White, Biomacromolecules **5**, 463 (2004).
[8]T. N. Nguyen, A. Rangel, and V. Migonney, Polym. Degrad. Stab. **176**, 109154 (2020).
[9]J. Z. Luk, J. Cooper-White, L. Rintoul, E. Taran, and L. Grøndahl, J. Mater. Chem. B **1**, 4171 (2013).
[10]G. Marletta, G. Ciapetti, C. Satriano, S. Pagani, and N. Baldini, Biomaterials **26**, 4793 (2005).
[11]K. Gross, J. K. Venkatesan, C. Falentin-Daudré, C. Vaquette, V. Migonney, and M. Cucchiarini, Osteoarthr. Cartil. **28**, S520 (2020).
[12]J. O. Jeong, S. I. Jeong, J. S. Park, H. J. Gwon, S. J. Ahn, H. Shin, J. Y. Lee, and Y. M. Lim, RSC Adv. **7**, 8963 (2017).
[13]A. Yeo, W. J. Wong, and S. H. Teoh, J. Biomed. Mater. Res. Part A **93**, 1358 (2010).
[14]A. L. Mutch, and L. Grondahl, Biointerphases **15**, 061006 (2018).
[15]Z. Yang, M. Zhengwei, S. Huayu, and G. Changyou, Sci. China Chem. **55**, 2419 (2012).
[16]Amélie Leroux, Tuan Nguyen, André Rangel, Isabelle Cacciapuoti, Delphine Duprez, David G. Castner, and Véronique Migonney, Biointerphases **15**, 061006 (2020).
[17]D. Hegemann, I. Indutnyi, L. Zajíčková, E. Makhneva, Z. Farka, Y. Ushenin, and M. Vandenbossche, Plasma Processes Polym. **15**, 1800090 (2018).
[18]M. Drabik, D. Lohmann, J. Hanus, A. Shelemin, P. Rupper, H. Biederman, and D. Hegemann, Plasma **1**, 156 (2018).
[19]L. Lee, K. Y. Cooper-White, J. J. Keen, and I. Grøndahl, *Tissue Enineering: Roles Materials and Applications*, edited by S. J. Barnes and L. P. Harris (Nova, New York, 2008).
[20]F. Cheng, L. J. Gamble, and D. G. Castner, Anal. Chem. **80**, 2564 (2008).
[21]D. G. Castner, Biointerphases **12**, 02C301 (2017).
[22]M. Xu, C. Guo, H. Dou, Y. Zuo, Y. Sun, J. Zhang, and W. Li, Polym. Chem. **10**, 3786 (2019).
[23]E. Vey, C. Roger, L. Meehan, J. Booth, M. Claybourn, A. F. Miller, and A. Saiani, Polym. Degrad. Stab. **93**, 1869 (2008).
[24]C. X. F. Lam, D. W. Hutmacher, J.-T. Schantz, M. A. Woodruff, and S. H. Teoh, J. Biomed. Mater. Res. Part A **90A**, 906 (2009).
[25]L. Grøndahl and J. Z. Luk, *Biointerfaces: Where Materials Meets Biology*, edited by D. M. Hutmacher and W. Chrzanowski (The Royal Society of Chemistry, Cambridge, 2014) pp. 312
[26]T. D. Brown, P. D. Dalton, and D. W. Hutmacher, Adv. Mater. **23**, 5651 (2011).
[27]D. K. Gilding and A. M. Reed, Polymer **20**, 1459 (1979).
[28]R. A. Jain, Biomaterials **21**, 2475 (2000).
[29]W. Friess and M. Schlapp, J. Pharm. Sci. **91**, 845 (2002).
[30]J. Z. Luk, J. Cork, J. Cooper-White, and L. Grøndahl, Langmuir **31**, 1746 (2015).
[31]A. K. Biswas, M. R. Islam, Z. S. Choudhury, A. Mostafa, and M. F. Kadir, Adv. Nat. Sci. Nanosci. Nanotechnol. **5**, 043001 (2014).
[32]E. Hewitt, S. Mros, M. Mcconnell, J. D. Cabral, and A. Ali, Biomed. Mater. **4**, 055013 (2019).
[33]N. Abbasi, S. Ivanovski, K. Gulati, R. M. Love, and S. Hamlet, Biomater. Res. **24**, 2 1 (2020).
[34]P. B. Warren, Z. G. Davis, and M. B. Fisher, J. Mech. Behav. Biomed. Mater. **99**, 153 (2019).
[35]D. Gupta, A. K. Singh, N. Kar, A. Dravid, and J. Bellare, Mater. Sci. Eng. C **98**, 602 (2019).
[36]L. A. Bosworth, W. Hu, Y. Shi, and S. H. Cartmell, J. Nanomater. **2019**, 1–11 (2019).
[37]A. C. Doty, Y. Zhang, D. G. Weinstein, Y. Wang, S. Choi, W. Qu, S. Mittal, and S. P. Schwendeman, Eur. J. Pharm. Biopharm. **113**, 24 (2017).
[38]M. Ghezzi, S. C. Thickett, A. M. Telford, C. D. Easton, L. Meagher, and C. Neto, Langmuir **30**, 11714 (2014).
[39]G. Schliecker, C. Schmidt, S. Fuchs, and T. Kissel, Biomaterials **24**, 3835 (2003).
[40]S. K. Sahoo, J. Panyam, S. Prabha, and V. Labhasetwar, J. Controlled Release **82**, 105 (2002).
[41]K. Khare, J. Zhou, and S. Yang, Langmuir **25**, 12794 (2009).
[42]S. Yang, K. Khare, and P. C. Lin, Adv. Funct. Mater. **20**, 2550 (2010).

[43]H. S. Kim and A. J. Crosby, Adv. Mater. **23**, 4188 (2011).
[44]M. Guvendiren, S. Yang, and J. A. Burdick, Adv. Funct. Mater. **19**, 3038 (2009).
[45]E. Makhneva, L. Barillas, K.-D. Weltmann, and K. Fricke, Biointerphases **15**, 061001 (2020).
[46]C. Neto, Phys. Chem. Chem. Phys. **9**, 149 (2007).
[47]R. Xie, A. Karim, J. F. Douglas, C. C. Han, and R. A. Weiss, Phys. Rev. Lett. **81**, 1251 (1998).
[48]E. V. Giger, B. Castagner, and J. Leroux, J. Controlled Release **167**, 175 (2013).
[49]E. S. Permyakova, J. Polčak, P. V. Slukin, S. G. Ignatov, N. A. Gloushankova, L. Zajíčková, D. V. Shtansky, and A. Manakhov, Mater. Des. **153**, 60 (2018).
[50]H. Otsuka, Y. Nagasaki, and K. Kataoka, Biomacromolecules **1**, 39 (2000).
[51]M. T. Zumstein, H. P. E. Kohler, K. McNeill, and M. Sander, Environ. Sci. Technol. **50**, 197 (2016).
[52]G. Gyulai, C. B. Pénzes, M. Mohai, T. Lohner, P. Petrik, S. Kurunczi, and T. E. Kiss, J. Colloid Interface Sci. **362**, 600 (2011).
[53]S. V. Anantakrishnan and R. V. Venkataratnam, Proc. Indian Acad. Sci. Sect. A **66**, 40 (1967).
[54]See supplementary material at http://dx.doi.org/10.1116/6.0000687 for DLS intensity based particle size distributions (Figure S1 and S2); AFM data for thickness estimation of PLGA film (Figure S3); XPS data of PLGA film (Figure S4); PCL film and disk AFM and SEM data (Figure S5); XPS of grafted PCL films and disks (Figure S6); XPS data of PCL scaffold samples (Figure S7); SEM data of PCL scaffold samples (Figure S8).